HHS Public Access

Author manuscript

Clin Cancer Res. Author manuscript; available in PMC 2017 June 01.

Published in final edited form as:

Clin Cancer Res. 2016 December 01; 22(23): 5805–5817. doi:10.1158/1078-0432.CCR-15-3051.

Therapeutic benefit of selective inhibition of p110α PI3-kinase in pancreatic neuroendocrine tumors

Adriana Soler[1], **Ana M Figueiredo**[1], **Pau Castel**[2], **Laura Martin**[3], **Erika Monelli**[1], **Ana Angulo-Urarte**[1], **Maria Milà-Guasch**[1], **Francesc Viñals**[3,4], and **Oriol Casanovas**[3]

[1]Vascular Signaling Laboratory, Institut d´Investigació Biomèdica de Bellvitge (IDIBELL), Gran Via de l'Hospitalet 199-203, 08907 L´Hospitalet de Llobregat, Barcelona, Spain

[2]Human Oncology and Pathogenesis Program (HOPP), Memorial Sloan Kettering Cancer Center, 1275 York Avenue, New York, NY 10065, USA

[3]Translational Research Laboratory, Catalan Institute of Oncology, IDIBELL, Gran Via de l'Hospitalet 199-203, 08907 L´Hospitalet de Llobregat, Barcelona, Spain

[4]Departament de Ciències Fisiològiques II, Universitat de Barcelona, 08907 L´Hospitalet de Llobregat, Spain

[5]Department of Medicine, Memorial Sloan Kettering Cancer Center, 1275 York Avenue, New York, NY 10065

Abstract

Purpose—Mutations in the PI3-kinase (PI3K) pathway occur in 16% of patients with pancreatic neuroendocrine tumors (PanNETs), which suggests that these tumors are an exciting setting for PI3K/AKT/mTOR pharmacological intervention. Everolimus, an mTOR inhibitor, is being used to treat patients with advanced PanNETs. However, resistance to mTOR targeted therapy is emerging partially due to the loss of mTOR-dependent feedback inhibition of AKT. In contrast, the response to PI3K inhibitors in PanNETs is unknown.

Experimental Design—In the present study, we assessed the frequency of PI3K pathway activation in human PanNETs and in RIP1-Tag2 mice, a preclinical tumor model of PanNETs, and we investigated the therapeutic efficacy of inhibiting PI3K in RIP1-Tag2 mice using a combination of pan (GDC-0941) and p110α selective (GDC-0326) inhibitors and isoform specific PI3K kinase-dead mutant mice.

Results—Human and mouse PanNETs showed enhanced pAKT, pPRAS40 and pS6 positivity compared to normal tissue. While treatment of RIP1-Tag2 mice with GDC-0941 led to reduced tumor growth with no impact on tumor vessels, the selective inactivation of the p110α PI3K isoform, either genetically or pharmacologically, reduced tumor growth as well as vascular area.

CORRESPONDENCE: Mariona Graupera: mgraupera@idibell.org, Vascular Signaling Laboratory, Institut d´Investigació Biomèdica de Bellvitge (IDIBELL), Gran Via de l'Hospitalet 199-203, 08907 L´Hospitalet de Llobregat, Barcelona, Spain, Tel: + 34 932 607 404, Fax: + 34 932 607 460.

Author contributions: AS, PC, MG and OC designed research, analyzed data and wrote the paper; AS, AMF, AAU, LM, PC performed research, FV analyzed data, and LF and JB provided reagents.

Conflict of interest: The authors of this manuscript do not have potential conflict of interests.

Furthermore, GDC-0326 reduced the incidence of liver and lymph node (LN) metastasis compared to vehicle treated mice. We also demonstrated that tumor and stromal cells are implicated in the anti-tumor activity of GDC-0326 in RIP1-Tag2 tumors.

Conclusion—Our data provide a rationale for p110α selective intervention in PanNETs and unravel a new function of this kinase in cancer biology through its role in promoting metastasis.

Introduction

Neuroendocrine tumors (NETs) comprise a family of malignancies that arise from neuroendocrine cells in different body locations (1). Fully-differentiated NETs are further classified as either carcinoid or pancreatic. In particular, pancreatic neuroendocrine tumors (PanNETs) have a low incidence rate (less than 0.5%) (2) but account for the second most prevalent malignancy of the pancreas (2–4). Despite being rare, PanNETs are often diagnosed at an advanced stage with a high proportion exhibiting metastatic lesions. The poor clinical response to current treatments, particularly after failure to respond to chemotherapy (5), highlights the need for new therapeutic options in the management of this tumor type.

PI3Ks are a family of lipid kinases composed of eight catalytic isoforms and grouped in three classes on the basis of structure, regulation, and preferred lipid substrate (6, 7). Mammals have four catalytic class I PI3K isoforms (p110α, p110β, p110γ and p110δ) which are constitutively bound to a regulatory subunit (6, 7). The AKT and mTOR axis is the major downstream hub of class I PI3K signaling, and mediates multiple cellular functions, including cell metabolism, growth, proliferation, migration, and survival (8).

Activation of the PI3K pathway is frequently observed in human cancer, as a consequence of multiple molecular alterations, including mutations (*PIK3CA*, *AKT1*, *PTEN, RAS*), gene amplification (*PIK3CA*, *AKT1*, *AKT2*), loss of expression of tumor suppressors (*PTEN*, *TSC2* and *INPP4B*), and oncogenic tyrosine kinase signaling (7, 9). PI3Ks also mediate tumor stromal functions, such as angiogenesis and recruitment of inflammatory cells (7, 10). A recent whole exome sequencing study has revealed mutations in PI3K pathway genes in 16% of patients with PanNETs (11); including mutations in *PIK3CA*, *PTEN*,and *TSC2*. In addition to mutations, PTEN and TSC2 expression levels are downregulated in 75% of PanNETs and is associated with reduced disease-free progression and overall survival (12). Furthermore, high activation of mTOR downstream effectors, such as pS6K and pS6 is associated with adverse clinical outcomes in PanNETs (13). Taken together, these data suggest that the PI3K/AKT/mTOR pathway might be functionally relevant in the progression of PanNETs and indicate that it is an exciting setting to test PI3K/AKT/mTOR pharmacological intervention. Indeed, everolimus, an mTOR allosteric inhibitor is currently being used to treat patients with advanced PanNETs (5, 14, 15). A phase II clinical trial has showed efficacy of everolimus in metastatic PanNETs after failure of chemotherapy (5, 15). More recently, the results of a first-line phase III trial with everolimus (RADIANT-3) have emerged (16). While the data did not show statistical differences, it is noteworthy that everolimus treatment resulted in a median overall survival of 44 months with a clinically substantial improvement of at least 6 months vs. placebo (16). A mechanism of adaptive

resistance to mTOR inhibitor has been described, involving loss of mTOR-dependent feedback inhibition of AKT (17–19). These data suggest that targeting PI3K, the upstream signal, may overcome this feedback loop. However, it is not currently known whether PI3K intervention in PanNETs results in an improved clinical outcome.

One of the most widely used models to study PanNETs is the genetically engineered RIP1-Tag2 model in which mice synchronously progress from incipient neoplasia to invasive carcinomas (20). Tumors of RIP1-Tag2 mice develop from the β-cells of the pancreatic of Langerhans islets as a result of expression of the SV40 large and small T-antigen under the control of the insulin promoter (20). Some evidence suggests that the PI3K pathway might be relevant during tumor progression in the RIP-Tag2 model (2). While specific inhibitors of mTOR have been tested in this preclinical model of PanNET progression, the effect of targeting PI3K isoforms is unknown (2).

Motivated by the observation that the PI3K pathway is often mutated and activated in PanNETs, we sought to investigate the therapeutic benefit of inhibiting the PI3K pathway in the RIP1-Tag2 mouse model. Here, we report that selective inactivation of the p110α isoform is sufficient to block RIP1-Tag2 tumor progression and metastasis. We demonstrate that inhibition of p110α impacts on tumor cells by inducing cell death and on the tumor microenvironment by compromising vessel growth.

Material and Methods

Mice

Mice were kept in individually-ventilated cages and cared for according to the guidelines and legislation of the Catalan DARP (Departament d' Agricultura, Ramaderia i Pesca). Heterozygous $p110\alpha^{D933A/WT}$ (Ref (21)), $p110\beta^{D931A/WT}$ (Ref (22)), and $p110\delta^{D910A/WT}$ (Ref (23)), RIP1-Tag2 (Ref(20)) were backcrossed onto the C57/BL6 background for >10 generations and WT littermates used as controls.

Cell lines

βTC3 and βTC4 cells were derived from RIP1-Tag2 mouse tumors (20). They were generated in Douglas Hanahan's laboratory in 1988 as previously described (24). Briefly, β cells were isolated by mechanical disruption from the tumor capsule and plated in 12-well plates in the presence of DMEM medium containing 15% horse serum, 2.5% fetal bovine serum and 25 mM glucose (24). We authenticated these cells every time that they were thawed by Insulin, large T antigen immunofluorescence and growth pattern and morphology.

Therapeutic treatments

RIP1-Tag2 mice were treated daily by oral gavage starting at 12 weeks of age until 14 weeks of age with GDC-0941 (100 mg/kg/day), GDC-0326 (12 mg/kg/day) or vehicle (0.5% (w/v) methylcellulose and 0.2% (w/v) polysorbate 80 in de-ionized water).

Metastasis Analysis

The presence of tumor cells in the liver or LNs was assessed by T-antigen immunostaining in either OCT embedded and frozen or fixed in 4% PFA and embedded in paraffin. The incidence of liver/LN metastasis was determined by scoring for presence or absence in each animal from a minimum of ten mice per group.

Statistical Analysis

Means were compared between two groups using nonparametric Mann Whitney's test and parametric t-student. For evaluating the Kaplan-Meier survival curves, Log Rank test was used. In all cases *$p < 0.05$, **$p < 0.01$, and ***$p < 0.001$ were considered statistically significant.

Results

PI3K pathway activation in human and mouse PanNETs

In order to study the frequency of PI3K pathway activation in human PanNETs, we stained tissue samples from normal pancreas (n=15) and tumors (n=40) from patients diagnosed with neuroendocrine islet cell tumors, with the phospho-specific antibodies pAKT (S473), pPRAS40 (T246) and pS6 (S240/4) that are widely used makers of PI3K/AKT/mTOR pathway activation. Normal tissue showed positive staining in the acinar cells of the pancreas and a lack of staining in the endocrine islet cells or Langerhans islets (Fig. 1A, left panel). In contrast, in the tumor cohort we found a variety of immunoreactivity across the samples ranging from negative to positive (Figure 1A, right panels). We found pAKT (S473) and pPRAS40 (T246) positivity in 15/40 cases (37.5%), and pS6 (S240/4) positivity in 16/40 cases (40%) (Fig. 1B). This finding was consistent with the heterogeneous nature of this disease, since many genetic drivers have been found to be responsible for the pathogenesis of human PanNETs.

To further explore our results in a preclinical model of PanNET, we took advantage of the RIP1-Tag2 mouse model of neuroendocrine tumor progression (from normal islet to invasive carcinoma). We speculated that the PI3K/AKT/mTOR pathway might be gradually activated during this process. Therefore, we stained pAKT (S473), pPRAS40 (T246), and pS6 (S240/4) in normal islets, encapsulated low-grade tumors, and invasive carcinomas from the RIP1-Tag2 mouse model. Consistent with our findings in human samples, exocrine structures were positive for all three stainings, while the endocrine islets were largely negative (Fig. 1C, top panels). Encapsulated tumors exhibited positivity for pAKT (S473), pPRAS40 (T246), and pS6 (S240/4) markers (Fig. 1C, middle panels). Remarkably, invasive tumors showed enhanced staining for all of the three markers of PI3K/AKT/mTOR pathway activation (Fig. 1C, bottom panels). Together, our results confirm the importance of the PI3K/AKT/mTOR signaling in the human pathology and during the progression of the PanNETs (13).

We next asked whether over-activation of the PI3K pathway in the human PanNET cohort and in the RIP1-Tag2 mouse tumor model was caused by loss of PTEN expression or by oncogenic activatory mutations in *PIK3CA*, the gene encoding p110α, two common

mechanisms by which PI3K signaling is activated in transformed cells (7). The majority of human tumors analyzed were positive for PTEN expression (Supplementary Fig. 1A and B). In the same line, encapsulated and invasive RIP1-Tag2 tumors, as well as βTC3 cells, a cell line derived of the RIP1-Tag2 model (25), showed positivity for PTEN (Supplementary Fig. 1C and D). Analysis of the three most prevalent hotspot mutations of *Pik3ca* (E542K/E545K and H1047R) by Sanger sequencing in βTC3 cells revealed that these cells did not contain mutated p110α (Supplementary Fig. 1E). Together these results suggest that over-activation of the PI3K pathway in the RIP1-Tag2 mouse model is not induced by either loss of expression of PTEN or oncogenic mutations in *PIK3CA*. Given that the SV40 T-antigens induced-PanNETs progressively activate EGFR signaling pathway, it is tempting to speculate that this mechanism accounts for activation of PI3K and its downstream effectors in the RIP1-Tag2 mouse model (2). Another possibility is that SV40 small T-antigen stimulates phosphorylation of AKT in a PP2A-dependent manner, as it has been reported in other systems (26).

Inhibition of PI3K blocks tumor progression in RIP1-Tag2 mice

Next, we tested the effect of inhibiting the PI3K signaling pathway *in vivo* by using the GDC-0941 compound (27), which inhibits p110α/β/γ and δ. As shown in Fig. 2A, administration of GDC-0941 to RIP1-Tag2 mice resulted in reduced AKT phosphorylation, suggesting inhibition of PI3K signaling. To test the impact of GDC-0941 on tumor progression, we focused on the initial onset of malignant progression (20, 25) (Supplementary Fig. 2A). We initiated daily treatment of 12-week-old RIP1-Tag2 animals, which corresponds to the timing of early tumor initiation, and continued the treatment until 14 weeks of age, when end-stage tumors are already present. Tumor-bearing RIP1-Tag2 mice treated with GDC-0941 showed a significant improvement in lifespan (Fig. 2B) with a trend towards decreased tumor burden (Fig. 2C) compared to control age-matched vehicle-treated animals.

We sought to analyze phenotypic markers of PI3K inhibition, including the proliferative status of tumor cells, microhaemorrhaging and vascular density of the tumor. GDC-0941 did not modify tumor cell proliferation *in vivo* (as assessed by Ki67 immunostaining; Supplementary Fig. 2B,C) indicating that PI3K signaling does not mediate this biological function in PanNETs. We validated this result in two cell lines derived of the RIP1-Tag2 model, the βTC3 and βTC4 cells (25). Pre-treatment with pan or isoform selective PI3K inhibitors did not alter βTC3 and βTC4 cell proliferation (Supplementary Fig. 2D-F). We further demonstrated the lack of effect of PI3K inhibition on cell proliferation of βTC3 and βTC4 cells by using BKM120, another pan-PI3K inhibitor (Supplementary Fig. 2E,F) (28).

In vivo treatment with GDC-0941 led to a minor reduction in the number of red tumors (Fig. 2D,E), suggesting an impact on tumor vasculature, in accordance with previous findings (10, 29). However, histological analysis of tumor vessels by CD31 staining and quantification showed that GDC-0941 did not modify vessel area (Fig. 2F,G).

Genetic inactivation of p110α impairs tumor growth in RIP1-Tag2 mice

To gain insight into the biochemical role of PI3K in PanNETs, we next studied whether different PI3K isoforms have selective roles in mediating PI3K signaling in the RIP1-Tag2 tumor model. βTC3 cells expressed p110α, p110β and p110δ, but not p110γ (Fig. 3A). Treatment of βTC3 cells with GDC-0941 and with GDC-0326, a newly developed small molecule inhibitor with selectivity for p110α inhibitor (Supplementary Fig. 3A) (30) reduced AKT phosphorylation (Fig. 3B), to a similar extent as BYL719, another selective p110α inhibitor (Supplementary Fig. 3B) (31). Conversely, the p110β selective inhibitor (TGX-221) or p110δ selective inhibitor (IC87114) failed to reduce pAKT levels in these cells (Fig. 3B), suggesting that the p110α PI3K isoform is principally responsible for activation of AKT in the RIP1-Tag2 mouse model.

To further address the role of individual p110 isoforms in tumor formation in the RIP1-Tag2 mice, we took advantage of knock-in (KI) mouse lines in which the endogenous p110α/β/δ isoforms have been converted to kinase-dead proteins ($p110\alpha^{D933A}$, $p110\beta^{D931A}$, and $p110\delta^{D910A}$) (21–23) by introducing a germline point mutation in the ATP-binding DFG motif of *Pik3ca* (gene encoding p110α), *Pik3cb* (gene encoding p110β), and *Pik3cd* (gene encoding p110δ Fig. 3C-E). These constitutive mutant mice mimic, to some extent, the effects of systemic administration of isoform selective PI3K inhibitors (22, 32, 33). Given that homozygous $p110\alpha^{D933A/D933A}$ and $p110\beta^{D931A/D931A}$ KI mice die during embryonic development (21, 22), we crossed heterozygous $p110\alpha^{D933A/WT}$, $p110\beta^{D931A/WT}$, and $p110\delta^{D910A/WT}$ (WT is the wild-type allele; Fig. 3C-E) with RIP1-Tag2 mice (further referred to as RIP1-Tag2-$p110\alpha^{D933A/WT}$, RIP1-Tag2-$p110\beta^{D931A/WT}$, and RIP1-Tag2-$p110\delta^{D910A/WT}$). Of note, the heterozygous p110 kinase-dead mutants have been crucial in understanding the physiological roles of these isoforms as they show an intermediate phenotype in cultured cells and in mice compared to homozygous mutants, indicating a dose-dependent activity of these PI3K isoforms (22, 32, 33).

To evaluate the effects of individual p110 isoforms on tumor initiation and growth, RIP1-Tag2-$p110\alpha^{D933A/WT}$, RIP1-Tag2-$p110\beta^{D931A/WT}$, and RIP1-Tag2-$p110\delta^{D910A/WT}$ mice were sacrificed at 14 weeks of age and compared to their WT littermates. No difference in overall survival was observed upon heterozygous genetic inactivation of p110α, p110β or p110δ, (Supplementary Fig. 3C). Instead, total mean tumor volume was blunted (by approximately 40%) upon inactivation of p110α (Fig. 3F) with no difference upon inactivation of p110β (Fig. 3G) and p110δ (Fig. 3H). Analysis of downstream PI3K signaling in individual RIP1-Tag2 tumors revealed reduced AKT phosphorylation and reduced mTORC1 signaling in RIP1-Tag2-$p110\alpha^{D933A/WT}$ (Fig. 3I,J). Conversely, inactivation of p110β and p110δ did not reduce AKT or S6 phosphorylation (Fig. 3K-N). Taken together, our data suggest that p110α, but not p110β and p110δ, activity contributes to PanNET progression in the RIP1-Tag2 mouse model. The lack of significance in tumor burden between wild-type and $p110\alpha^{D933A/WT}$ tumors is likely due to the heterozygous approach used.

p110α gene inactivation blocks tumor angiogenesis

Phenotypic analysis of individual tumors revealed that constitutive heterozygous genetic inactivation of p110α, p110β and p110δ did not alter the number of proliferative tumor cells (Supplementary Fig. 3D). Given the relevant role of p110α in tumor angiogenesis (29), we hypothesized that the anti-tumor activity of p110α inactivation may relate to alterations in the tumor vasculature. Indeed, p110α$^{D933A/WT}$ tumors exhibited reduced vascular area (Fig. 4A,B). Consistent with no role of p110β and p110δ in developmental angiogenesis (33), RIP1-Tag2-p110β$^{D931A/WT}$ and RIP1-Tag2-p110δ$^{D910A/WT}$ had a similar CD31 positive area compared to their WT littermates (Fig. 4C-F). To further demonstrate a role for p110α in tumor angiogenesis, we macroscopically assessed the number of hypervascularized “red islets” with dilated, micro-hemorrhaging vasculature. RIP1-Tag2-p110α$^{D933A/WT}$ pancreases showed a reduced number of red islets (Supplementary Fig. 4A). Interestingly, RIP1-Tag2-p110β$^{D931A/WT}$ and RIP1-Tag2-p110δ$^{D910A/WT}$ tumors also showed reduced number of red islets (Supplementary Fig. 4B,C), and although the reason for this effect is not clear, it might be related to additional stromal functions previously attributed to these isoforms (10, 34). Taken together, our data suggest that the anti-tumor activity observed upon inactivation of p110α is due to its effect on vessel growth.

Selective pharmacological inactivation of p110α leads to a positive therapeutic response

The genetic analysis using PI3K kinase-dead mice promoted us to further investigate the selective inhibition of p110α using a pharmacological strategy, which allows the inhibition of this isoform at a greater level. We first tested whether inhibition of p110α alone was sufficient to abrogate PI3K/AKT signaling both *in vitro* and *in vivo*. Treatment with GDC-0326 abolished AKT phosphorylation in βTC3 cells (Fig. 3B) and in RIP1-Tag2 tumors (Fig. 5A). Next, tumor-bearing RIP1-Tag2 mice were treated with GDC-0326 from week 12 of age to week 14 of age. A significant improvement in the lifespan of RIP1-Tag2 mice was observed upon GDC-0326 treatment compared to control age-matched mice treated with vehicle (Fig. 5B). Furthermore, GDC-0326 produced a significant impairment in tumor growth (approximately 60% reduction; Fig. 5C). To further investigate the response to selective p110α inhibition, we assessed incidence of tumor dissemination and metastasis in peripancreatic LNs and liver. The presence of tumor cells in LNs and liver was detected by H&E and T antigen immunostaining (Fig. 5D). Remarkably, none of the GDC-0326 treated RIP1-Tag2 mice showed positivity for Anti-T antigen in the liver (Fig. 5E,F). Quantification of incidence of microscopic LN metastasis revealed that the presence of tumor cells in LNs was reduced by four times in GDC-0326-treated animals compared to controls (Fig. 5E,F). Furthermore, from those mice that showed LN infiltration, the average number of positive nodes was also decreased upon selective inhibition of p110α (1.6±0.78 vs. 1 ± 0 number of positive T antigen LN /animal). Taken together, our data suggest that selective inhibition of p110α in the RIP1-Tag2 mouse model blocks tumor cell dissemination.

GDC-0326 blocks tumor growth principally by inhibiting angiogenesis

Analysis for phenotypic markers of the PI3K inhibition revealed that GDC-0326 did not alter tumor cell proliferation *in vivo* (Supplementary Fig. 5A,B). Conversely, inhibition of

p110α led to reduced number of “red islet” (Fig. 6A) and decreased vascular area (Fig. 6B,C) suggesting anti-angiogenic activity of GDC-0326. The impact of PI3K inhibitors on tumor vessels has been attributed to reduced VEGF levels and to direct cell-autonomous effects on endothelial cells (ECs) (10, 29). Analysis of mRNA levels of VEGF in RIP1-Tag2 tumors revealed no difference between vehicle and GDC-0326 treated tumors (Supplementary Fig. 5C). Instead, incubation of mouse lung ECs with GDC-0326 resulted in reduced cell migration with no effect on cell proliferation and survival (Supplementary Fig. 6), as previously shown (33, 35). Together these data suggest that the anti-vascular effects induced by GDC-0326 in RIP1-Tag2 mice are mainly EC-mediated.

Previous data from our laboratory have shown that stromal inhibition of p110α results in reduced vessel function, which in turn leads to tumor cell death (29). RIP1-Tag2 mice treated with GDC-0326 showed an overall increase in tumor cell-death assessed by TUNEL staining (Fig. 6D,E). We assessed whether this apoptotic effect was cell intrinsic or stromal mediated. Pre-treatment of βTC3 cultured cells with GDC-0326 resulted in increased apoptosis (Fig. 6F). Of note, pre-treatment of βTC3 cells with p110β and p110δ selective inhibitors did not induce cell death (Fig. 6F). These data suggest that treatment with GDC-0326 leads to tumor cell-death by at least partially stimulating apoptosis directly on these cells. We next assessed whether GDC-0326 pro-apoptotic effects were enhanced in low nutrients conditions. Treatment of βTC3 and βTC4 cells with GDC-0326 and BYL719 under low glucose conditions also stimulated cell death (Supplementary 6D,F) to a similar extent than normal growing conditions. Taken together, these data demonstrate tumor cell intrinsic cytotoxic properties of PI3K inhibitors in βTC3 and βTC4 cells, albeit at low levels. Our data further suggest that tumor-cell death induced by selective inhibition of p110α *in vivo* is principally mediated by reduced vascularity.

Discussion

PanNETs are considered rare tumors with low incidence, but with high prevalence among pancreatic tumors (1, 3, 36). This type of neoplasm comprises a highly heterogeneous disease, which has complicated the development of targeted therapies. Recent advances in the understanding of molecular alterations in PanNETs have allowed the identification of the relevant mechanisms involved in the pathogenesis of this neoplasm. The PI3K/AKT/mTOR pathway is mutated in 16% of PanNETs, and therefore presents an exciting therapeutic target (11). *PIK3CA* is frequently amplified or somatically mutated in solid tumors (7), which has encouraged a tremendous drug development effort to target this isoform. Indeed, there are numerous ongoing clinical trials assessing different compounds to target the PI3K pathway, including those that specifically interfere with the p110α isoform (9, 37). However, it is still under debate which type of inhibitor (pan-PI3K inhibitor vs. isoform-selective PI3K inhibitor) would offer a better clinical outcome. Pan-PI3K inhibitors may exhibit higher toxicity, especially when combined with other agents. Isoform selective inhibitors may instead show less efficacy or increased compensations by other PI3K isoforms (7, 9). Using a combination of unique genetic and novel pharmacologic tools, we show here that p110α mediates PI3K signaling in PanNETs and demonstrate that selective inhibition of p110α is sufficient to block PanNET progression. Hence, our data provide for the first time the rational to selectively target this isoform in this malignancy. Of note, further clinical

investigation is warranted to address whether these compound would be useful in the clinical setting and whether the therapeutic benefit for p110α inhibitors is justified considering toxicities observed in early clinical trials (hyperglycemia, gastrointestinal issues, and skin rash) (7).

Under the setting in which we analyzed the anti-tumor effect of selective p110α inhibition in the RIP1-Tag2 model, no resistance to treatment was observed. Interestingly, resistance to p110α inhibitors is related to loss of PTEN, which in turn results in p110β dependency (31). The observation that inhibition of all class I isoforms results in a similar anti-tumor response as selective inhibition of p110α in the RIP1-Tag2 model further supports the lack of resistance to the p110α inhibitor and no tumoral effects mediated by p110β. However, it remains to be elucidated whether long-term treatment of RIP1-Tag2 tumors with p110α selective inhibitors gives rise to resistance to treatment.

Our data support a dual anti-tumor effect of p110α intervention in PanNETs, namely anti-vascular and pro-apoptotic, with the stromal effects being more prominent. p110α signaling is essential for blood vessels to grow in development and in tumors (29, 33). Therefore, p110α signaling in the endothelium is expected to account for tumor angiogenesis in PanNETs. PI3K signaling also promotes tumor angiogenesis by stimulating VEGF expression in tumor cells (10). Although VEGF is highly expressed in RIP1-Tag2 tumors (25), we have found that selective inhibition of p110α does not interfere with VEGF mRNA levels in these tumors. Together, our findings suggest that p110α activity stimulates tumor angiogenesis in RIP1-Tag2 tumors by regulating EC biology in a cell autonomous manner.

Selective inhibition of p110α also results in tumor cell death both *in vivo* and *in vitro*. Albeit significant, the impact of GDC-0326 on tumor cells *in vitro* is modest, which suggests that the apoptotic effect in the tumor observed *in vivo* upon GDC-0326 treatment is principally due to the reduction in tumor vascularity. Of note, this pro-apoptotic effect was confirmed by using BYL719, a p110α selective inhibitor currently being tested in the clinic for breast, head and neck and gastrointestinal tumors (7). Interestingly, traditional anti-angiogenic agents also lead to increased tumor cell death with no impact on tumor cell proliferation in RIP1-Tag2 tumors (38). In line with previous studies that treated RIP1-Tag2 mice with the mTOR inhibitor rapamycin (2), our results do not support a role for PI3K signaling in tumor cell proliferation. Our data differ from the findings of Valentino et al. (39) that showed that human neuroendocrine cells treated with BKM120, a pan PI3K inhibitor induced cell death and cell cycle arrest. Although, the reasons for these discrepancies are not clear at the moment, they may relate to the use of different doses of BKM120. Of note, when used at high doses (>1 μM), BKM120 shows some off-target effects, namely inhibiting microtubule polymerization. (40), which may explain why this compound inhibited cell proliferation.

An intriguing result of our study was that inhibiting all class I PI3K isoforms in RIP1-Tag2 mice did not impact on tumor angiogenesis. This is surprising given that tumor cells express all class I PI3K isoforms and therefore redundancy function of PI3K isoforms in oncogenic signaling was expected, as has been documented in other tumor systems (7, 41). Class I PI3K isoforms have, however, pleiotropic roles in cancer which include both cancer intrinsic and extrinsic (stromal) functions, which underscores the complexity of targeting this

pathway in cancer (7, 10). The different angiogenic response observed upon GDC-0941 (Fig. 2) vs. GDC-0326 (Fig. 6) in RIP1-Tag2 mice may thus relate to compensatory effects which result from inhibiting all class I PI3K isoforms (10, 34).

An important finding of our study is that p110α inhibition blocks tumor cell dissemination. Hyperactivation of PI3K/AKT has been associated with increased invasion, metastasis and poor prognosis (42, 43). Consistently, recent data have identified the PI3K/AKT hub as a key mediator of metastatic cancer development by regulating epithelial-mesenchymal transition (44). However, it is still unknown which PI3K isoform mediates this process. Our findings identify, for the first time, that the p110α isoform is a key mediator of tumor metastasis *in vivo*. This is in agreement with previous data, which showed that p110α regulates migration of metastatic tumor cells *in vitro* (45). Although the mechanism through which inhibition of p110α impedes metastasis *in vivo* it is not clear at the moment, it might relate to its effects on the tumor vessels. However, we cannot rule out that p110α may also regulate tumor cell intrinsic effects required for successfully colonization of secondary sites such as motility, polarity and strong survival capabilities (46). Further studies are warranted to mechanistically elucidate how p110α regulates tumor dissemination. Given that PanNETs are often diagnosed with metastatic disease, it would be relevant to also test whether targeting p110α can also inhibit an established metastatic lesion. Another interestingly unexplored aspect in this context would be to assess the effect of selective p110α targeting in cancer initiating cells.

The results of a phase III trial in PanNETs with everolimus have recently emerged showing beneficial effects but lacking statistical power (16), highlighting the need to continued need to improve therapies. Our data strongly indicate that p110α inhibition could be an alternative therapy to overcome limitations associated with everolimus. In addition to cell intrinsic tumor effects, targeting p110α in PanNETs also compromises tumor angiogenesis. In contrast, rapamycin treatment in RIP1-Tag2 mouse does not impact on tumor vessels which suggest reduced anti-tumor activity compared to treatment with p110α inhibitor. (2). Furthermore, PI3K acts upstream of mTOR and its inhibition may overcome mTOR-dependent feedback inhibition of AKT (17–19). In a scenario of complete blockade of PI3K/AKT, residual mTORC1 activity is enough to reduce the anti-tumor activity of p110α inhibition. Therefore, it is tempting to speculate that a combination of p110α and mTOR inhibitors in the treatment of PanNETs may cooperate to enhance the effectiveness of each compound alone. In line with this, combined RAD001 (rapalogue) and BEZ235 (a dual mTOR/PI3K inhibitor) treatment of neuroendocrine tumor cells *in vitro* overcomes resistance to RAD001 (47). Sunitinib, a tyrosine kinase inhibitor, is another targeted therapy currently being used in the clinic in PanNET patients. Mechanistically, sunitinib blocks, amongst others, VEGF signaling and in turn leads to vascular trimming and a delay in tumor progression (48). However, this inhibition is also accompanied by increased tumor dissemination in some preclinical tumor models, including PanNETs (49, 50), and effect that is overcome by c-Met inhibition (50). Based on the observation that PI3K signaling is activated downstream of c-Met, together with our data showing that selective inhibition of p110α inhibits metastasis, it is tempting to speculate that simultaneous inhibition of p110α and VEGF in PanNETs may also overcome limitations of VEGF targeted therapy.

In conclusion, our work provides insights from mouse genetic and pharmacological studies to be translated into human therapy. Given that the RIP1-Tag2 tumor model used in this study has shown predictive value in demonstrating the clinical activity of targeted therapies, including everolimus and sunitinib (2, 25, 49), our data provide the rationale for the use of a p110α selective inhibitor to treat this disease.

Supplementary Material

Refer to Web version on PubMed Central for supplementary material.

Acknowledgments

We thank Alba Martinez (Research Laboratory, Catalan Institute of Oncology, IDIBELL, Barcelona), and Mar Martinez for support with experiments. We thank Lori Friedman Department of Cancer Signaling, Genentech, Inc., South San Francisco, CA, USA) for GDC-0326. We thank Maria Whitehead, UCL cancer Institute, UCL for critical review of the manuscript. We thank Douglas Hanahan for kindly providing βTC3 and βTC4 cells.

Grant Support

Work in MG's laboratory is supported by research grants SAF2013-46542-P and SAF2014-59950-P from MINECO (Spain), 2014-SGR-725 from the Catalan Government, the People Programme (Marie Curie Actions; grant agreement 317250) of the European Union's Seventh Framework Programme FP7/2007-2013/, the Marie Skłodowska-Curie (grant agreement 675392) of the European Union's Horizon 2020 research and innovation programme, the Institute of Health Carlos III (ISC III) and the European Regional Development Fund (ERDF) under the integrated Project of Excellence no. PIE13/00022 (ONCOPROFILE). Work in OC's laboratory is supported by ERC starting grant (ERC-STG-281830). Personal support was from FPI of the Spanish Ministry of Education (A.S.), Marie-Curie ITN Actions (A.M.F. and E.M.) and Ramon y Cajal fellow of the Spanish Ministry of Education (M.G. and O.C.).

References

1. Yao JC, Hassan M, Phan A, Dagohoy C, Leary C, Mares JE, et al. One hundred years after "carcinoid": epidemiology of and prognostic factors for neuroendocrine tumors in 35,825 cases in the United States. J Clin Oncol. 2008; 26:3063–3072. [PubMed: 18565894]
2. Chiu CW, Nozawa H, Hanahan D. Survival benefit with proapoptotic molecular and pathologic responses from dual targeting of mammalian target of rapamycin and epidermal growth factor receptor in a preclinical model of pancreatic neuroendocrine carcinogenesis. J Clin Oncol. 2010; 28:4425–4433. [PubMed: 20823411]
3. Modlin IM, Lye KD, Kidd M. A 5-decade analysis of 13,715 carcinoid tumors. Cancer. 2003; 97:934–959. [PubMed: 12569593]
4. Ekeblad S, Skogseid B, Dunder K, Oberg K, Eriksson B. Prognostic factors and survival in 324 patients with pancreatic endocrine tumor treated at a single institution. Clin Cancer Res. 2008; 14:7798–7803. [PubMed: 19047107]
5. Yao JC, Lombard-Bohas C, Baudin E, Kvols LK, Rougier P, Ruszniewski P, et al. Daily oral everolimus activity in patients with metastatic pancreatic neuroendocrine tumors after failure of cytotoxic chemotherapy: a phase II trial. J Clin Oncol. 2010; 28:69–76. [PubMed: 19933912]
6. Vanhaesebroeck B, Guillermet-Guibert J, Graupera M, Bilanges B. The emerging mechanisms of isoform-specific PI3K signalling. Nat Rev Mol Cell Biol. 2010; 11:329–341. [PubMed: 20379207]
7. Fruman DA, Rommel C. PI3K and cancer: lessons, challenges and opportunities. Nat Rev Drug Discov. 2014; 13:140–156. [PubMed: 24481312]
8. Manning BD, Cantley LC. AKT/PKB signaling: navigating downstream. Cell. 2007; 129:1261–1274. [PubMed: 17604717]
9. Rodon J, Dienstmann R, Serra V, Tabernero J. Development of PI3K inhibitors: lessons learned from early clinical trials. Nat Rev Clin Oncol. 2013; 10:143–153. [PubMed: 23400000]

10. Soler A, Angulo-Urarte A, Graupera M. PI3K at the crossroads of tumour angiogenesi signaling pathways. Molecular and Cellular Oncology. 2015; 2 e975624-1:10.
11. Jiao Y, Shi C, Edil BH, de Wilde RF, Klimstra DS, Maitra A, et al. DAXX/ATRX, MEN1, and mTOR pathway genes are frequently altered in pancreatic neuroendocrine tumors. Science. 2011; 331:1199–1203. [PubMed: 21252315]
12. Missiaglia E, Dalai I, Barbi S, Beghelli S, Falconi M, della Peruta M, et al. Pancreatic endocrine tumors: expression profiling evidences a role for AKT-mTOR pathway. J Clin Oncol. 2010; 28:245–255. [PubMed: 19917848]
13. Qian ZR, Ter-Minassian M, Chan JA, Imamura Y, Hooshmand SM, Kuchiba A, et al. Prognostic significance of MTOR pathway component expression in neuroendocrine tumors. J Clin Oncol. 2013; 31:3418–3425. [PubMed: 23980085]
14. Chan J, Kulke M. Targeting the mTOR signaling pathway in neuroendocrine tumors. Curr Treat Options Oncol. 2014; 15:365–379. [PubMed: 25092520]
15. Yao JC, Shah MH, Ito T, Bohas CL, Wolin EM, Van Cutsem E, et al. Everolimus for advanced pancreatic neuroendocrine tumors. N Engl J Med. 2011; 364:514–523. [PubMed: 21306238]
16. Yao JP, M. Lombard-Bochas C, van Cutsem E, Lam D, Kunz T, Brandt U, Capdevila J, De Vries E, Hobday T, Tomassetti P, Pommier R. Everolimus (EVE) for the treatment of advanced pancreatic neuroendocrine tumours (pNET): final overall survival (OS) results of a randomized, double-blind, placebo (PBO)-controlled multicenter phase III trail (RADIANT-3). Ann Oncol. 2014; 25(suppl4):iv394–iv405.
17. O'Reilly KE, Rojo F, She QB, Solit D, Mills GB, Smith D, et al. mTOR inhibition induces upstream receptor tyrosine kinase signaling and activates Akt. Cancer Res. 2006; 66:1500–1508. [PubMed: 16452206]
18. Sun SY, Rosenberg LM, Wang X, Zhou Z, Yue P, Fu H, et al. Activation of Akt and eIF4E survival pathways by rapamycin-mediated mammalian target of rapamycin inhibition. Cancer Res. 2005; 65:7052–7058. [PubMed: 16103051]
19. Carracedo A, Ma L, Teruya-Feldstein J, Rojo F, Salmena L, Alimonti A, et al. Inhibition of mTORC1 leads to MAPK pathway activation through a PI3K-dependent feedback loop in human cancer. J Clin Invest. 2008; 118:3065–3074. [PubMed: 18725988]
20. Hanahan D. Heritable formation of pancreatic beta-cell tumours in transgenic mice expressing recombinant insulin/simian virus 40 oncogenes. Nature. 1985; 315:115–122. [PubMed: 2986015]
21. Foukas LC, Claret M, Pearce W, Okkenhaug K, Meek S, Peskett E, et al. Critical role for the p110alpha phosphoinositide-3-OH kinase in growth and metabolic regulation. Nature. 2006; 441:366–370. [PubMed: 16625210]
22. Guillermet-Guibert J, Smith LB, Halet G, Whitehead MA, Pearce W, Rebourcet D, et al. Novel Role for p110beta PI 3-Kinase in Male Fertility through Regulation of Androgen Receptor Activity in Sertoli Cells. PLoS Genet. 2015; 11:e1005304. [PubMed: 26132308]
23. Okkenhaug K, Bilancio A, Farjot G, Priddle H, Sancho S, Peskett E, et al. Impaired B and T cell antigen receptor signaling in p110delta PI 3-kinase mutant mice. Science. 2002; 297:1031–1034. [PubMed: 12130661]
24. Efrat S, Linde S, Kofod H, Spector D, Delannoy M, Grant S, et al. Beta-cell lines derived from transgenic mice expressing a hybrid insulin gene-oncogene. Proc Natl Acad Sci U S A. 1988; 85:9037–9041. [PubMed: 2848253]
25. Casanovas O, Hicklin DJ, Bergers G, Hanahan D. Drug resistance by evasion of antiangiogenic targeting of VEGF signaling in late-stage pancreatic islet tumors. Cancer Cell. 2005; 8:299–309. [PubMed: 16226705]
26. Rodriguez-Viciana P, Collins C, Fried M. Polyoma and SV40 proteins differentially regulate PP2A to activate distinct cellular signaling pathways involved in growth control. Proc Natl Acad Sci U S A. 2006; 103:19290–19295. [PubMed: 17158797]
27. Edgar KA, Wallin JJ, Berry M, Lee LB, Prior WW, Sampath D, et al. Isoform-specific phosphoinositide 3-kinase inhibitors exert distinct effects in solid tumors. Cancer Res. 2010; 70:1164–1172. [PubMed: 20103642]

28. Burger MT, Pecchi S, Wagman A, Ni ZJ, Knapp M, Hendrickson T, et al. Identification of NVP-BKM120 as a Potent, Selective, Orally Bioavailable Class I PI3 Kinase Inhibitor for Treating Cancer. ACS Med Chem Lett. 2011; 2:774–779. [PubMed: 24900266]
29. Soler A, Serra H, Pearce W, Angulo A, Guillermet-Guibert J, Friedman LS, et al. Inhibition of the p110alpha isoform of PI 3-kinase stimulates nonfunctional tumor angiogenesis. J Exp Med. 2013; 210:1937–1945. [PubMed: 24043760]
30. Heffron TP, Heald RA, Ndubaku C, Wei B, Augistin M, Do S, et al. The Rational Design of Selective Benzoxazepin Inhibitors of the alpha-Isoform of Phosphoinositide 3-Kinase Culminating in the Identification of (S)-2-((2-(1-Isopropyl-1H-1,2,4-triazol-5-yl)-5,6-dihydrobenzo[f]imidazo[1,2-d][1,4]oxazepin-9-yl)oxy)propanamide (GDC-0326). J Med Chem. 2016; 59:985–1002. [PubMed: 26741947]
31. Juric D, Castel P, Griffith M, Griffith OL, Won HH, Ellis H, et al. Convergent loss of PTEN leads to clinical resistance to a PI(3)Kalpha inhibitor. Nature. 2015; 518:240–244. [PubMed: 25409150]
32. Bilancio A, Okkenhaug K, Camps M, Emery JL, Ruckle T, Rommel C, et al. Key role of the p110delta isoform of PI3K in B-cell antigen and IL-4 receptor signaling: comparative analysis of genetic and pharmacologic interference with p110delta function in B cells. Blood. 2006; 107:642–650. [PubMed: 16179367]
33. Graupera M, Guillermet-Guibert J, Foukas LC, Phng LK, Cain RJ, Salpekar A, et al. Angiogenesis selectively requires the p110alpha isoform of PI3K to control endothelial cell migration. Nature. 2008; 453:662–666. [PubMed: 18449193]
34. Rivera LB, Meyronet D, Hervieu V, Frederick MJ, Bergsland E, Bergers G. Intratumoral myeloid cells regulate responsiveness and resistance to antiangiogenic therapy. Cell Rep. 2015; 11:577–591. [PubMed: 25892230]
35. Herbert SP, Huisken J, Kim TN, Feldman ME, Houseman BT, Wang RA, et al. Arterial-venous segregation by selective cell sprouting: an alternative mode of blood vessel formation. Science. 2009; 326:294–298. [PubMed: 19815777]
36. Capdevila J, Meeker A, Garcia-Carbonero R, Pietras K, Astudillo A, Casanovas O, et al. Molecular biology of neuroendocrine tumors: from pathways to biomarkers and targets. Cancer Metastasis Rev. 2014; 33:345–351. [PubMed: 24375391]
37. Weigelt B, Downward J. Genomic Determinants of PI3K Pathway Inhibitor Response in Cancer. Front Oncol. 2012; 2:109. [PubMed: 22970424]
38. Bergers G, Javaherian K, Lo KM, Folkman J, Hanahan D. Effects of angiogenesis inhibitors on multistage carcinogenesis in mice. Science. 1999; 284:808–812. [PubMed: 10221914]
39. Valentino JD, Li J, Zaytseva YY, Mustain WC, Elliott VA, Kim JT, et al. Cotargeting the PI3K and RAS pathways for the treatment of neuroendocrine tumors. Clin Cancer Res. 2014; 20:1212–1222. [PubMed: 24443523]
40. Brachmann SM, Kleylein-Sohn J, Gaulis S, Kauffmann A, Blommers MJ, Kazic-Legueux M, et al. Characterization of the mechanism of action of the pan class I PI3K inhibitor NVP-BKM120 across a broad range of concentrations. Mol Cancer Ther. 2012; 11:1747–1757. [PubMed: 22653967]
41. Foukas LC, Berenjeno IM, Gray A, Khwaja A, Vanhaesebroeck B. Activity of any class IA PI3K isoform can sustain cell proliferation and survival. Proc Natl Acad Sci U S A. 2010; 107:11381–11396. [PubMed: 20534549]
42. Perez-Tenorio G, Stal O. Activation of AKT/PKB in breast cancer predicts a worse outcome among endocrine treated patients. Br J Cancer. 2002; 86:540–545. [PubMed: 11870534]
43. Vivanco I, Sawyers CL. The phosphatidylinositol 3-Kinase AKT pathway in human cancer. Nat Rev Cancer. 2002; 2:489–501. [PubMed: 12094235]
44. Xue G, Restuccia DF, Lan Q, Hynx D, Dirnhofer S, Hess D, et al. Akt/PKB-mediated phosphorylation of Twist1 promotes tumor metastasis via mediating cross-talk between PI3K/Akt and TGF-beta signaling axes. Cancer Discov. 2012; 2:248–259. [PubMed: 22585995]
45. Qiao M, Iglehart JD, Pardee AB. Metastatic potential of 21T human breast cancer cells depends on Akt/protein kinase B activation. Cancer Res. 2007; 67:5293–5299. [PubMed: 17545609]
46. Yuan TL, Cantley LC. PI3K pathway alterations in cancer: variations on a theme. Oncogene. 2008; 27:5497–5510. [PubMed: 18794884]

47. Passacantilli I, Capurso G, Archibugi L, Calabretta S, Caldarola S, Loreni F, et al. Combined therapy with RAD001 e BEZ235 overcomes resistance of PET immortalized cell lines to mTOR inhibition. Oncotarget. 2014; 5:5381–5391. [PubMed: 25026292]

48. Raymond E, Dahan L, Raoul JL, Bang YJ, Borbath I, Lombard-Bohas C, et al. Sunitinib malate for the treatment of pancreatic neuroendocrine tumors. N Engl J Med. 2011; 364:501–513. [PubMed: 21306237]

49. Paez-Ribes M, Allen E, Hudock J, Takeda T, Okuyama H, Vinals F, et al. Antiangiogenic therapy elicits malignant progression of tumors to increased local invasion and distant metastasis. Cancer Cell. 2009; 15:220–231. [PubMed: 19249680]

50. Sennino B, Ishiguro-Oonuma T, Wei Y, Naylor RM, Williamson CW, Bhagwandin V, et al. Suppression of tumor invasion and metastasis by concurrent inhibition of c-Met and VEGF signaling in pancreatic neuroendocrine tumors. Cancer Discov. 2012; 2:270–287. [PubMed: 22585997]

Translational Relevance

PanNETs are heterogeneous tumors, which has complicated the design of targeted therapies. By using a preclinical mouse model of PanNET, we report here on a new therapy to treat this malignancy, namely selective inhibition of the class I p110α PI3K isoform, and demonstrate that targeting this isoform inhibits tumor progression and metastasis. This is particularly relevant given that isoform-selective PI3K inhibitors are likely to exhibit lower toxicity compared to pan-PI3K inhibitors, and therefore higher drug doses which achieve complete inhibition of the pathway are expected to be tolerated. We also observe that p110α signaling regulates tumor cell dissemination, which provides a significant advance in understanding the role of PI3K signaling in cancer and opens new therapeutic opportunities for agents targeting this pathway.

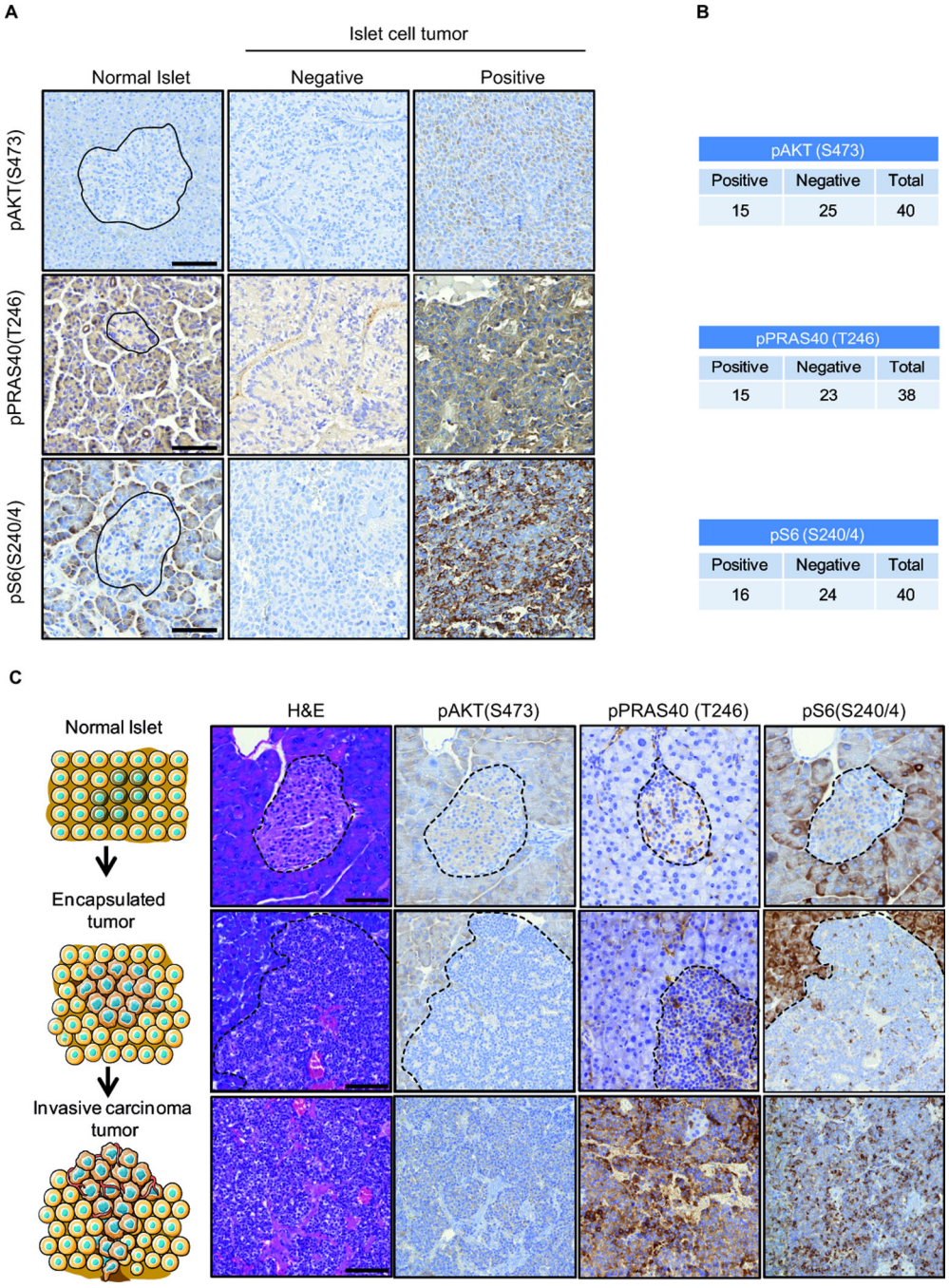

Figure 1. Activation of PI3K signaling in human and mouse PanNETs

A. Representative IHC images of human pancreatic islet cells, and neuroendocrine islet cell tumors for pAKT (S473) (above), pPRAS40 (T246) (middle) and pS6 (S240/4) (below) stainings. For islet cell tumors, representative negative and positive stainings are shown. Black lines delimit the normal islet. Scale bar: 100 μm. **B**. Quantification for the pAKT (S473), pPRAS40 (T246) and pS6 (S240/4) staining in a cohort of 40 human pancreatic neuroendocrine tumors. Black lines delimit the normal islet. **C**. Representative images of the RIP1-Tag2 mouse model normal islet cells, encapsulated pancreatic tumor, and invasive

carcinoma tumor stained with the PI3K pathway surrogates pAKT (S473), pPRAS40 (T246) and pS6 (S240/4). Dashed lines delimit the normal islet and the encapsulated tumor. Scale bar: 100 μm.

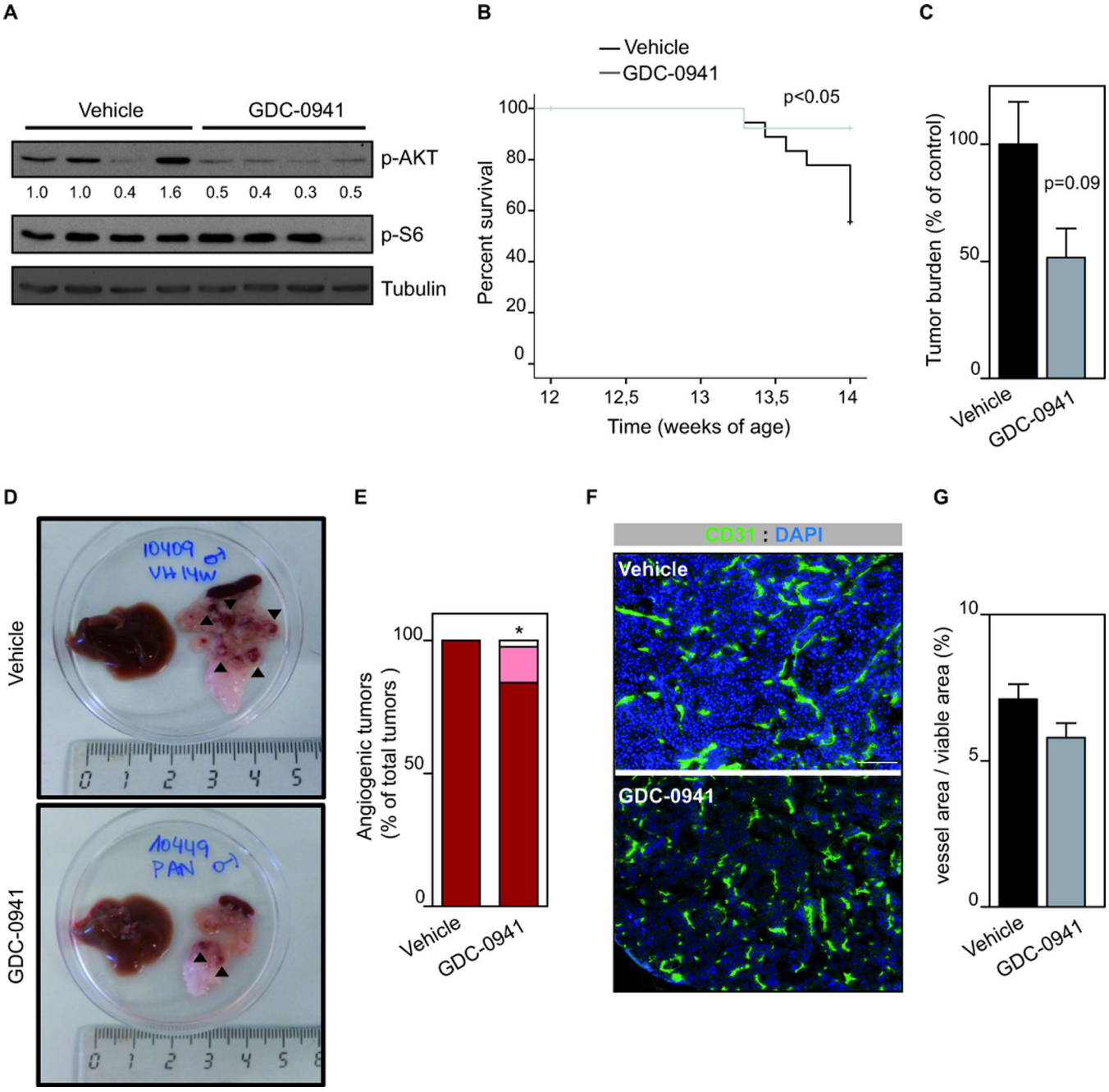

Figure 2. Inhibition of class I PI3K isoforms impairs tumor progression

A. Western blot of AKT and S6 phosphorylation in individual RIP1-Tag2 tumors treated with vehicle or GDC-0941 for 3 h. **B**. Kaplan-Meier survival curves in tumor-bearing RIP1-Tag2 mice (12 weeks) treated daily with vehicle (n=12) or GDC-0941 (100 mg/kg, n=12) for 2 weeks. **C**. Total tumor burden analysis in 2-week treatment trial with vehicle (n=27) or GDC-0941 (100 mg/kg, n=12) starting at 12 weeks of age until 14 weeks of age. **D**. Gross pathology images of excised pancreas and livers from animals treated with vehicle or GDC-0941 for 2 weeks. Black arrow heads indicate tumors. **E**. Quantification of number of angiogenic “red” islet per mouse in vehicle (n=12) or GDC-0941 (n=11) for 2 weeks. **F**.

CD31 and DAPI-stained sections of vehicle- or GDC-0941-treated RIP1-Tag2 tumors. Scale bar: 100 μm. **G**. The graph shows quantification of vessel area per tumor viable area of RIP1-Tag2 tumors treated with vehicle (n=8) or GDC-0941 (n=23). Error bars are standard error of the mean.

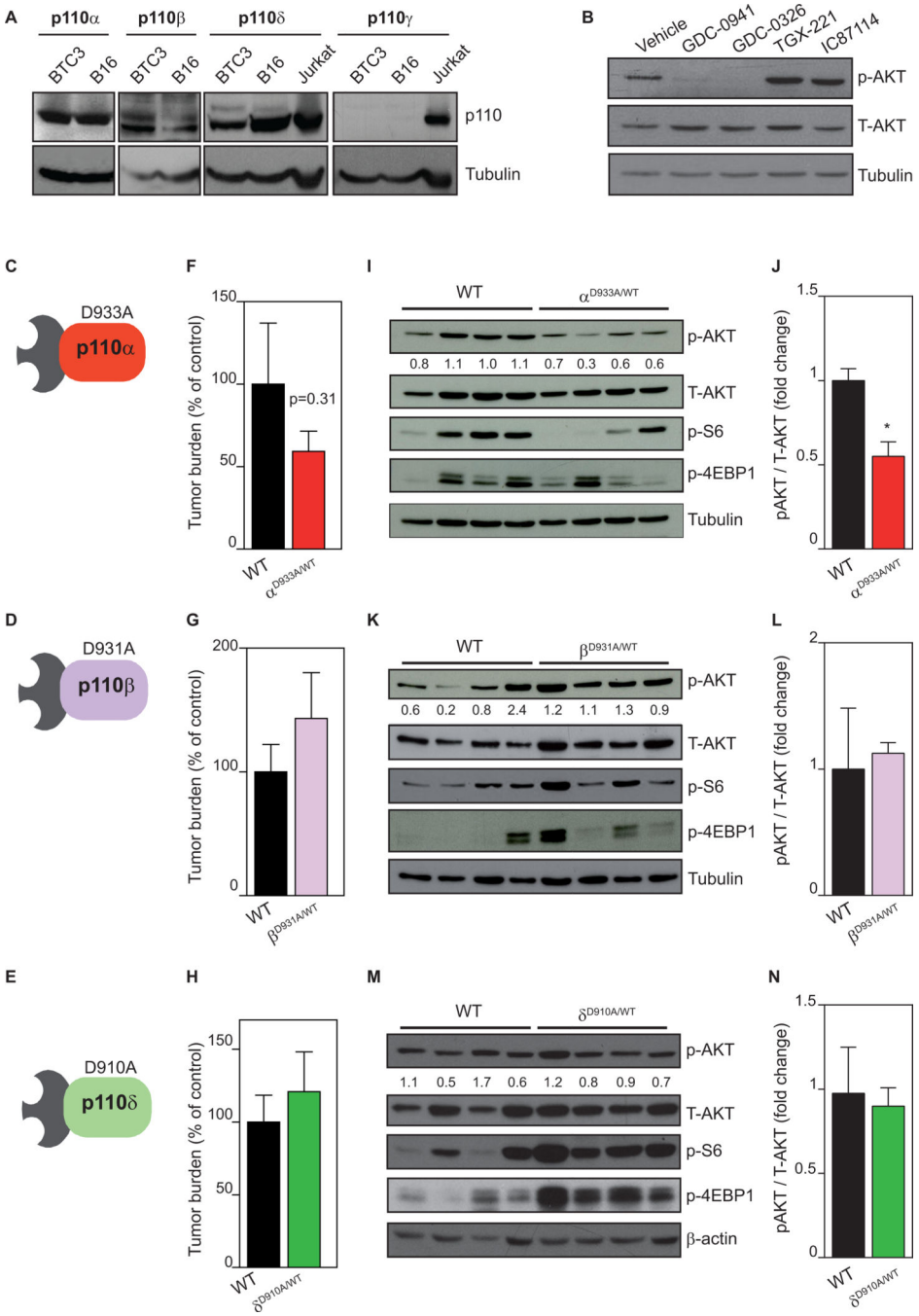

Figure 3. Genetic inactivation of p110α, but not p110β and p110δ, inhibits tumor growth

A. Analysis of p110 isoforms by western blot in βTC3 cells. B16 and Jurkat lysates were used as positive controls. **B**. Exponentially growing βTC3 cells were treated for 2 h with vehicle, GDC-0941 (1 μM), GDC-0326 (1 μM), TGX-221 (0.5 μM) or IC87114 (5 μM), followed by immunoblotting of total cell lysate using the indicated antibodies. **C**. Schematic illustration of the p110α$^{D933A/WT}$ mouse. **D**. Schematic illustration of the p110β$^{D931A/WT}$ mouse. **E**. Schematic illustration of the p110δ$^{D910A/WT}$ mouse. **F**. Total tumor burden analysis in WT (n=19) and p110α$^{D933A/WT}$ (n=18) littermates at 14 weeks of age. **G**. Total

tumor burden analysis in WT (n=10) and p110β$^{D931A/WT}$ (n=14) littermates at 14 weeks of age. **H**. Total tumor burden analysis in wild-type (n=9) and p110δ$^{D910A/WT}$ (n=24) littermates at 14 weeks of age. **I**. Western blot of AKT, S6 and 4EBP1 phosphorylation in individual RIP1-Tag2 tumors of WT and p110α$^{D933A/WT}$ littermates at 14 weeks of age. **J**. Bars show quantification of the relative immunoreactivity of pAKT normalized to total AKT. **K**. Western blot of AKT, S6 and 4EBP1 phosphorylation in individual RIP1-Tag2 tumors of WT and p110β$^{D931A/WT}$ littermates at 14 weeks of age. **L**. Bars show quantification of the relative immunoreactivity of pAKT normalized to total AKT. **M**. Western blot of AKT, S6 and 4EBP1 phosphorylation in individual RIP1-Tag2 tumors of wild-type and p110δ$^{D910A/WT}$ littermates at 14 weeks of age. **N**. Bars show quantification of the relative immunoreactivity of pAKT normalized to total AKT. Scale bar in A, C and E: 25 μm. Error bars are standard error of the mean.

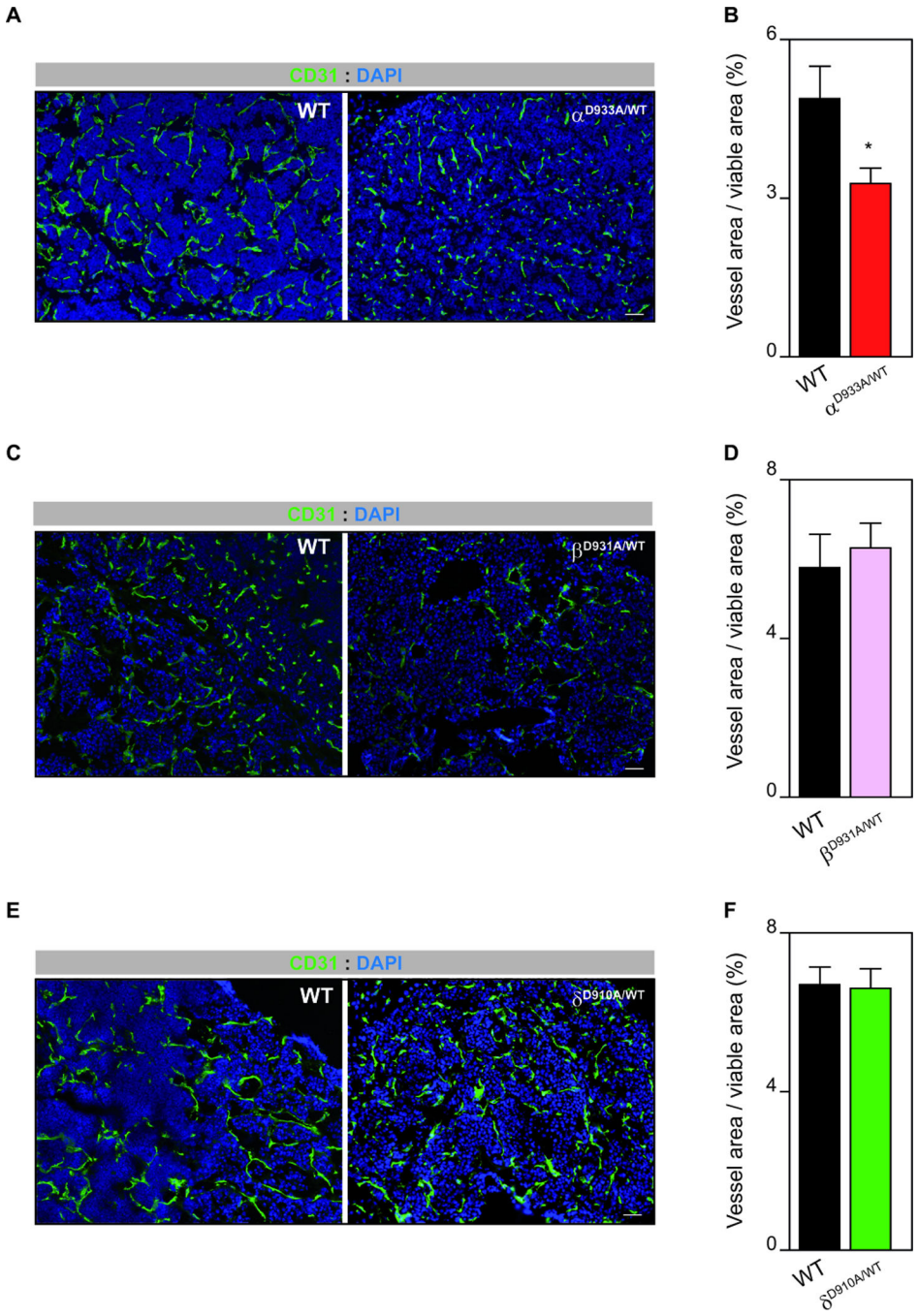

Figure 4. p110α signaling promotes tumor angiogenesis

A. CD31 and DAPI-stained sections of WT and p110α$^{D933A/WT}$ RIP1-Tag2 tumors. **B**. The graph shows quantification of vessel area per tumor viable area of WT (n=17) and p110α$^{D933A/WT}$ (n=10) RIP1-Tag2 tumors. **C**. CD31 and DAPI-stained sections of WT and p110β$^{D931A/WT}$ RIP1-Tag2 tumors. **D**. The graph shows quantification of vessel area per tumor viable area of WT (n=5) and p110β$^{D931A/WT}$ (n=10) RIP1-Tag2 tumors. **E**. CD31 and DAPI-stained sections of WT and p110δ$^{D910A/WT}$ RIP1-Tag2 tumors. **F**. The graph shows

quantification of vessel area per tumor viable area of WT (n=7) and p110δ$^{D910A/WT}$ (n=16) RIP1-Tag2 tumors. Error bars are standard error of the mean.

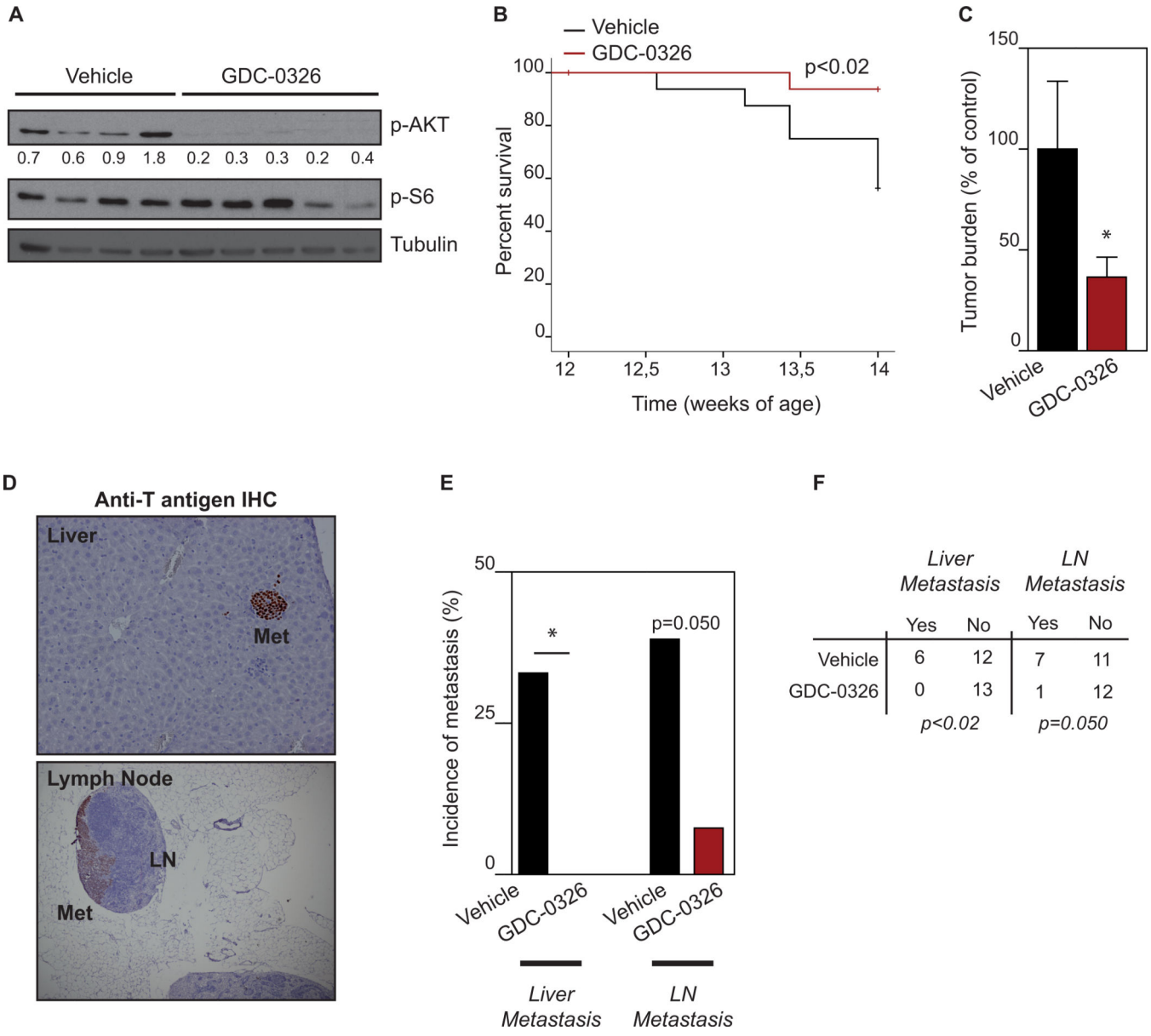

Figure 5. Pharmacological inhibition of p110α blocks tumor growth and metastasis

A. Western blot of AKT and S6 phosphorylation in individual RIP1-Tag2 tumors treated with vehicle or GDC-0326 for 3 h. **B**. Kaplan-Meier survival curves in tumor-bearing RIP1-Tag2 mice (12 weeks) treated daily with vehicle (n=13) or GDC-0326 (12 mg/kg, n=13) for 2 weeks. **C**. Total tumor burden analysis in 2-weeks treatment trial with vehicle (n=13) or GDC-0326 (12 mg/kg, n=13) starting at 12 weeks of age until 14 weeks of age. **D**. Histological analysis of liver and LN metastasis (Met) in RIP1-Tag2 mice treated with vehicle or GDC-0326 for 14 days starting at 12 weeks of age. Paraffin embedded sections were immunohistochemical stained for the tumor marker SV40 T antigen (brown). **E**. Quantification of the incidence of animals with microscopic liver micrometastasis and microscopic LN metastasis in the control (black bars) and GDC-0326 treated (red bars) treatment arms. **F**. Contingency table relating the number and percentage of animals in each

treatment/metastasis case. GDC-0326 treated mice show a statistic significant decrease in the incidence of liver micrometastasis and LN metastasis by the chi-square test.

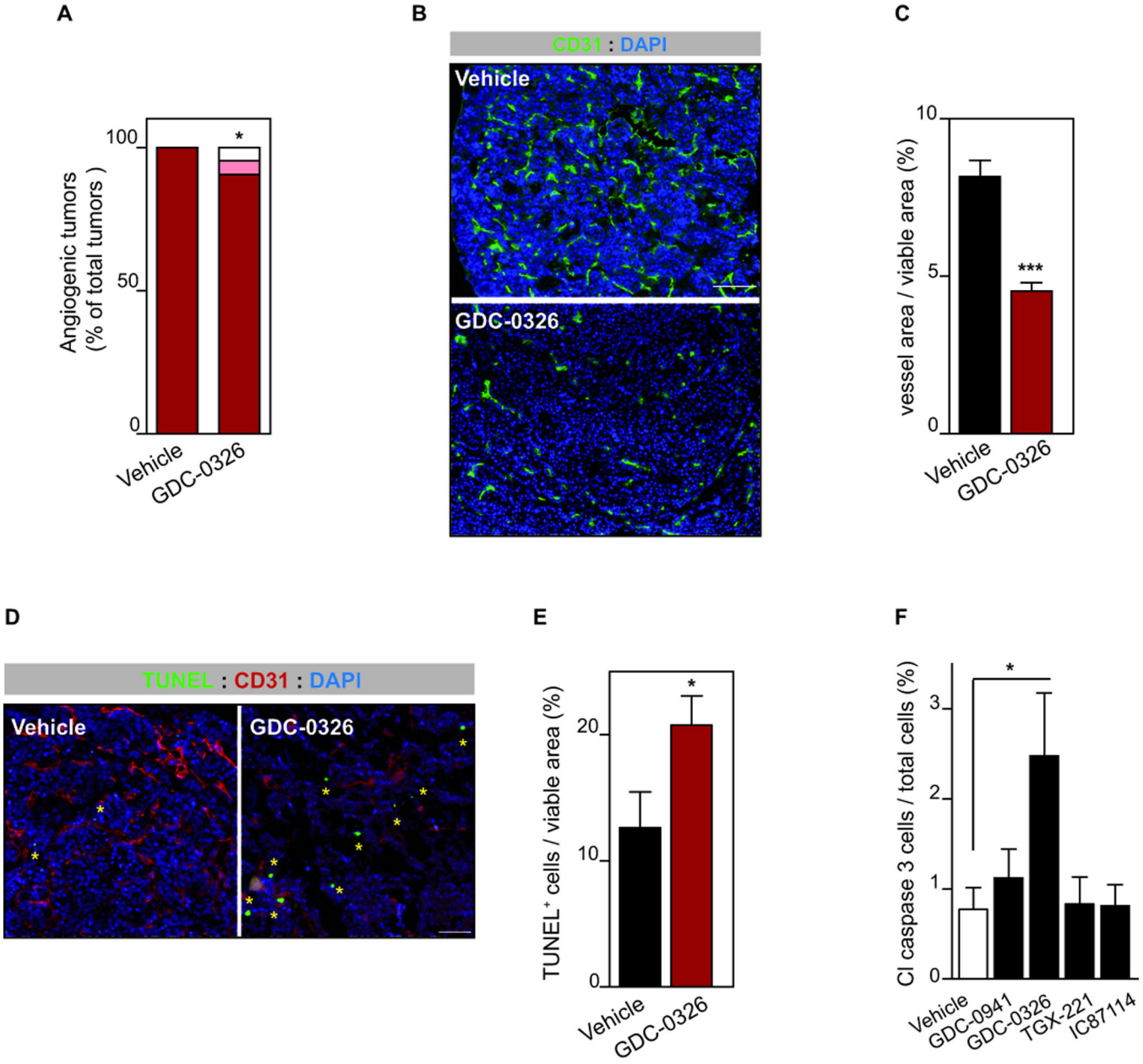

Figure 6. Inhibition of p110α results in cell intrinsic and extrinsic tumor effects

A. Quantification of number of angiogenic "red" islet per mouse in vehicle (n=13) or GDC-0326 (n=7) for 2 weeks. **B**. CD31 and DAPI-stained sections of vehicle- or GDC-0326-treated RIP1-Tag2 tumors. Scale bar: 100 μm. **C**. The graph shows quantification of vessel area per tumor viable area of RIP1-Tag2 tumors treated with vehicle (n=8) or GDC-0326- (n=22). **D**. Sections of tumors stained for TUNEL (green), CD31 (red) and DAPI (blue). Yellow asterisk marks TUNEL positive cells Scale bar: 50 μm. **E**. Bar graphs show quantification of apoptotic cells per viable tumor area in RIP1-Tag2 tumors treated with vehicle (n=10) or GDC-0326- (n=14). **E**. Cell viability of βTC3 cells following 48 h *in vitro* treatment with vehicle, GDC-0941 (1 μM), GDC-0326 (1 μM), TGX-221 (0.5

μM) or IC87114 (5 μM), and analyzed by cleaved-caspase-3 immunoflorescence. Mean of eight independent experiments is shown. Error bars are standard error of the mean.